16th World Conference on Earthquake, 16WCEE 2017
Santiago Chile, January 9th to 13th 2017
Paper N° 2133
Registration Code: S-O1463265100

INFLUENCE OF VISCOUS DAMPING MODELS ON INELASTIC SEISMIC RESPONSE OF FIXED AND BASE-ISOLATED STRUCTURES

A. Lanzi[(1),(2)], J. E. Luco[(3)]

[(1)] Department of Structural and Geothecnical Engineering, Sapienza Università di Roma, Rome, Italy
[(2)] General Direction for Dams, Ministry of Infrastructures and Transport, Rome, Italy, armando.lanzi@mit.gov.it
[(3)] Professor, Department of Structural Engineering, Jacobs School of Engineering, University of California, San Diego, La Jolla, CA, jeluco@ucsd.edu

Abstract

Work conducted over the last 30 years by a number of authors indicate that the details of the inherent damping model have a significant effect on the calculated inelastic structural response and, particularly, on the calculated damping forces. In some cases, unrealistically large damping forces can be obtained, which may imply unconservative results. Also, it is known that the mass-proportional term in the Rayleigh and Caughey damping matrices may be responsible for large damping forces for base-isolated or poorly constrained structures. In the absence of sufficient experimental data, there is a lack of consensus on the most appropriate model for inherent damping.

The first objective of the paper is to present and evaluate a new damping model in which the inherent damping force during inelastic vibrations is taken to be proportional to an estimate of the elastic component of velocity rather than to the total velocity which includes plastic and elastic components. This model has a number of theoretical and computational advantages. The second objective is to investigate the effect that different damping models, including models based on: (i) initial structural properties, (ii) degraded properties (tangent stiffness), and (iii) the new 'elastic' velocity model, have on the seismic response of fixed and base-isolated structures. In each case, three different estimates of the damping matrix are considered: (1) Rayleigh damping, (2) optimized Caughey series including and excluding the mass proportional term, and (3) modal damping matrix. The effects of different viscous damping models are quantified by numerical inelastic time-history analyses of a multi-story structure subjected to different earthquake excitations. The final objective is to study numerically whether a harmonic critical excitation exists for a multi-story structure supported on a bilinear hysteretic isolator system. This would extend previous analytical findings for a simple bilinear oscillator and for a 1-DOF structure resting on a bilinear hysteretic isolator, that even in the presence of hysteretic damping, a critical amplitude of the harmonic excitation exists, beyond which the resonant response of the structure can be unbounded (in absence of viscous damping) or very large (in presence of isolator damping).

Keywords: Viscous damping; non-linear analysis; base-isolation.

1. Introduction

1.1 Objectives of the Paper

The numerical solution of the equations of motion in structural dynamics requires assembling a damping matrix in addition to the standard mass matrix and a stiffness matrix which could be incremental. While in the linear case, and except for the conditions at resonance, the effects of damping are typically small, in the inelastic case the details of the inherent damping model have a significant effect on the structural response and, particularly, on the calculated damping forces. At the present time, a consensus has not developed with respect to the modeling of inherent damping (as opposed to the hysteretic damping resulting from inelastic action) in structures which experience significant inelastic response. A number of different modeling options involving Rayleigh, Caughey and modal viscous damping matrices based on initial or tangent properties have been proposed and warnings about unintended consequences of these choices have been voiced for the last 30 years by a number of authors (Crisp [1], Shing and Mahin [2], Leger and Dussault [3], Bernal [4], Carr [5],[6],[7], Hall [8], Ryan and Polanco [9], Charney [10], Petrini et al [11], Zareian and Medina [12], Smyrou et al [13], Jehel et al [14], Chopra and McKenna [15]). Some authors recommend to abandon altogether the use of a viscous damping matrix and to replace it by a hysteretic mechanism (e.g. Charney [10]) or by a capped model as proposed by Hall [8].

The first and primary objective of this paper is to present and evaluate a new damping model in which the inherent damping force during inelastic vibrations is taken to be proportional to an estimate of the elastic component of velocity rather than the total velocity which includes plastic and elastic components. This model has a number of theoretical and computational advantages. The second objective is to investigate the effect that different damping models, including models based on: (i) initial structural properties, (ii) degraded properties (tangent stiffness), and (iii) the new "elastic" velocity model, have on the seismic response of fixed and base-isolated structures. In each case, three different estimates of the damping matrix are considered: (1) Rayleigh damping, (2) the optimized Caughey series recently proposed by the authors, including and excluding the mass proportional term, and (3) modal damping matrix. The effects of different viscous damping models are quantified by numerical inelastic time-history analyses of a multi-story structure subjected to different earthquake excitations. Results in the form of peak displacements, velocities, damping forces, restoring forces, and energy dissipated by hysteretic action and inherent damping are presented. In the case of base-isolated structures, the evaluation of the effect of the mass-proportional term in Rayleigh and Caughey damping is of particular interest.

The final objective of the paper is to study numerically whether a harmonic critical excitation exists for a multi-story structure supported on a bilinear hysteretic isolator system. This would extend the analytical findings for a simple bilinear oscillator (Caughey, [16]) and for a 1-DOF structure resting on a bilinear hysteretic isolator (Luco, [17]), that even in the presence of hysteretic damping, a critical amplitude of the harmonic excitation exists, beyond which the resonant response of the structure can be unbounded (in absence of viscous damping) or very large (in presence of isolator damping). The role of viscous damping in the superstructure and isolator in limiting the response at the critical excitation is examined.

1.2 Summary of Methods to Calculate the Damping Matrix

Although not required by numerical solutions, a convenient choice for a damping matrix is to consider classical damping matrices which lead, in the linear case, to classical normal modes with prescribed modal damping ratios. Classical damping matrices based on initial properties are typically represented as Rayleigh, Caughey [18, 19], or modal damping matrices as obtained by Wilson and Penzien [20]. The simplest and most extensively used model is the Rayleigh damping matrix

$$[c] = \alpha[m] + \beta[k] \tag{1}$$

in which $[m]$ and $[k]$ are the mass and stiffness matrices, and α and β are coefficients determined by use of prescribed modal damping ratios at two selected modes or by a rule which attempts to minimize deviations over a frequency range (e.g. Hall [8]). The conceptual difficulties associated with the mass-proportional term and the potentially large damping ratios for the higher modes resulting from the stiffness-proportional term in Eq. (1) have been recognized for a long time (Crisp [1], Bernal [4], Carr [5], Hall [8], Ryan and Polanco [9], Charney [10]).

A more flexible but less frequently used approach to form a classical damping matrix is by use of Caughey series in terms of the stiffness matrix (Caughey [18]), or the flexibility matrix (Caughey and O'Kelly [19])

$$[c] = [m]\sum_{l=L}^{M+L-1} a_l \left([m]^{-1}[k]\right)^l \quad , \quad [c] = [m]\sum_{l=0}^{M-1} a_l \left([k]^{-1}[m]\right)^l \tag{2a,b}$$

In these equations M is the number of terms in the series and L=0 or L=1 depending on whether the mass term is included or excluded in Eq. (2a). The coefficients of the different terms in the Caughey series are determined by specifying the damping ratios at a set of natural frequencies or at judiciously selected pivot points. The resulting Vandermonde system of equations for the coefficients is notoriously ill-conditioned and leads to large fluctuations of the modal damping ratios at frequencies other than those at which the damping ratios are specified. Alternative and explicit forms for full or truncated Caughey series in terms of arbitrarily prescribed damping ratios at a set of natural frequencies have been obtained by the authors (Luco [21] for series 2a, and Lanzi and Luco [22] for series 2b). These explicit solutions circumvent the need to solve an ill-conditioned system of equations but require knowledge of a set of natural frequencies. Recently the authors (Luco and Lanzi [23], Lanzi and Luco [22]) have developed an optimized procedure to obtain the coefficients of the Caughey

series by a least squares fit between the polynomial representing the damping ratios and the assumed known frequency dependence of the damping ratios. They have also obtained alternative expansions of the damping matrix in terms of Legendre polynomials. The results do not require knowledge of the natural frequencies or mode shapes, lead to a classical damping matrix with stable damping ratios, and can be easily implemented by taking advantage of tables of optimized coefficients for Caughey series of different orders. The approach also allows the exclusion of the mass-proportional term from the series.

A third approach to obtain a classical damping matrix is the modal approach of Wilson and Penzien [20]

$$[c] = [m][\Phi]\, diag\,[2\omega_r \xi_r][\Phi]^T [m] = 2\sum_{r=1}^{M} (\omega_r \xi_r)[m]\{\phi^{(r)}\}\{\phi^{(r)}\}^T [m] \tag{3}$$

in which [Φ] is the matrix of eigen vectors normalized by the mass matrix. This procedure requires calculation of the mode shapes and natural frequencies and leads to zero damping for the modes for which the modal damping ratios are not specified. It should be noted that Eqs. (2a), (2b) and (3) lead to the same damping matrix if damping is specified at all modes. Finally, for the special case of uniform modal damping ratios, the following expressions (Luco [24] for Eq. (4a), Lanzi and Luco [22] for Eq. (4b))

$$[c] = 2\xi_0 [k]^{1/2} ([k]^{-1/2} [m][k]^{-1/2})^{1/2} [k]^{1/2} \quad , \quad [c] = 2\xi_0 [k]^{1/2} ([k]^{-1/2} [m][k]^{-1/2})^{1/2} [k]^{1/2} \tag{4a,b}$$

can be used to obtain classical damping matrices at the cost of calculating the square roots of the matrices indicated. Equation (4a) requires that the mass matrix be non-singular while Eq (4b) requires that the stiffness matrix be non-singular.

Bernal [4] has noted that the large "spurious" damping forces at massless degrees of freedom near yielding elements with high initial stiffness that arise from use of Rayleigh damping can be eliminated by use of Caughey damping with negative powers [Eq. (2b)], as the mass matrix appears as a factor pre- and post-multiplying another modal characteristic matrix. Carr [5] and Chopra and McKenna [15] have noted that the modal damping matrix [Eq. (3)] also has this property.

The very limited experimental data available seems to suggest that the inherent damping capacity also degrades as the structure degrades. Several of the models described above have been used or can be used in this fashion by replacing the initial stiffness matrix [k] by the tangent stiffness [k_t]. This extended practice is somewhat controversial. As noted by Charney [19], several academic structural analysis packages allow for this possibility while others do not allow or recommend it.

2. A Proposed New Model for Inherent Damping

As point of departure, we consider the linear elastic case in which the nodal viscous damping force vector $\{f_d\}$ is related to the velocity vector $\{\dot{u}\}$ by

$$\{f_d\} = [c]\{\dot{u}\} \tag{5}$$

in which [c] is the damping matrix. In this linear case, the displacement vector $\{u\}$ can be expressed in terms of the restoring force vector $\{f_s\}$ by $\{u\} = [k]^{-1}\{f_s\}$. Substitution of the corresponding velocity

$$\{\dot{u}\} = [k]^{-1}\{\dot{f}_s\} \tag{6}$$

into Eq. (5) leads to

$$\{f_d\} = [c][k]^{-1}\{\dot{f}_s\} \tag{7}$$

which relates the viscous damping force with the first derivative of the restoring force. At this point, we postulate that Eq. (7) will remain valid in the inelastic case with [k] and [c] being based on the initial structural

properties. In essence, this implies that the inherent damping force in the inelastic case is related to the estimate of "elastic" component of the velocity

$$\{\dot{u}_e\} = [k]^{-1}\{\dot{f}_s\} \tag{8}$$

and not to the total velocity. The damping model given by Eq. (7) complies with the expectations that: (i) the model should reduce to the standard viscous model in the linear case, (ii) the damping forces should be mostly associated with loading and unloading, (iii) the inherent damping should be clearly separated from the hysteretic damping due to inelastic action, and (iv) there should not be any remnant inherent damping force at the end of the structural motion. In addition, if the damping matrix [*c*] is based on Eq. (2b) as suggested by Bernal [4], or by the modal approach [Eq. (3)] as suggested by Carr [5] and Chopra and McKenna [15], or by use of Eq. (4b), then the damping forces at massless degrees of freedom would be zero.

It should be noted that for a simple bilinear oscillator, if the total displacement is written as $\Delta = u_p + u_e$, where u_p and u_e are the plastic and elastic displacements, respectively, then, at all points, $u_e = f_s / k_i$ where k_i is the initial stiffness. The resulting elastic velocity $\dot{u}_e = \dot{f}_s / k_i$ is consistent with Eq. (8). It is also interesting to note that in the particular case of a simple bilinear oscillator with stiffness proportional damping, the proposed model based on initial properties leads to the same result as those resulting from use of the conventional model with tangent stiffness. For the proposed model, assuming stiffness proportional damping $c = \beta k_i$ and $f_d = \beta k_i k_i^{-1} \dot{f}_s = \beta \dot{f}_s$. For the conventional tangent stiffness model, $f_d = \beta k_t \dot{\Delta}$ while loading or unloading with stiffness $k_t = k_i$, then $\dot{\Delta} = \dot{f}_s / k_i$ and $f_d = \beta \dot{f}_s$. During yielding with degraded stiffness $k_t = k_d$, then $\dot{\Delta} = \dot{f}_s / k_d$ and, again, $f_d = \beta \dot{f}_s$.

3. Effects of viscous damping models on a ten-story building

In order to investigate the effects of different viscous damping models on the calculated structural response, we performed a parametric study of the earthquake response of a ten-story building. The structure is represented by a fixed-base shear-type model, similar to that considered by Hall [8], having floor stiffness and strength that decrease with the height according to an assigned story-value vector {*SV*}

$$\{SV\}^T = (1.000, 0.984, 0.951, 0.902, 0.837, 0.755, 0.657, 0.542, 0.411, 0.264) \tag{9}$$

The numerical model consists of ten equal masses $m_i = m = 340 \cdot 10^3$ kg (i=1,10), interconnected by bilinear shear springs, each having an initial stiffness k_i, a yield strength F_{yi} and a degraded stiffness $k_{i,pl} = 0.10 \cdot k_i$. The initial stiffness of the first story $k_1 = 7.11 \cdot 10^5$ KN/m is selected so that the fundamental elastic period of the model is $T_1 = 1.0$ s, while the first-story yield strength is taken as 0.15 times the weight of the building $F_{y1} = 0.15 \cdot 10 \cdot mg = 5003$ KN. Initial stiffness and yield strength of the higher storeys are proportional to the story-value vector {*SV*} listed in Eq. (9), leading to a constant interstory yield displacement of 0.7 cm (assuming a story height of 4 m, the yield drift ratio is about 0.2%).

The inherent damping is represented by a viscous mechanism, characterized by a constant damping ratio $\xi_0 = 5\%$. A proportional damping matrix [*c*] is assembled by four different approaches: (1) by a Rayleigh damping matrix given by Eq. (1) where the coefficients $\alpha = 0.4523$ and $\beta = 0.0045$ are selected so that the modal damping ratios are equal to ξ_0 at the first two elastic natural frequencies; (2) by the modal damping matrix given by Eq. (3), calculated considering a constant damping ratio equal to ξ_0 for all modes; (3) by a 20th order Caughey series including the mass proportional term (labeled *LSQM*), obtained by use of the expansion in Legendre polynomials [as given by Eq. (29) with $M = 20$ in Ref. [23]]; (4) by a Caughey series obtained by use of the expansion in Legendre polynomials with $M = 20$ but excluding the mass proportional term (labeled *LSQK*) [i.e. by means of Eq. (29) in Ref. [23], with the coefficients b_n replaced by $\bar{b}_n$ given by Eq. (40)]. In the last two

approaches, the normalizing frequency $\omega_{\max}$ is selected to correspond to the highest initial natural frequency $\omega_{\max} = 85.36$ rad/s.

Table 1 lists the natural periods and frequencies of the elastic structure (T_i and f_i) as well as the damping ratios calculated by the different approaches. Table 1 also lists, for illustration, extreme estimates of the instantaneous natural periods and frequencies (*Tangent* values, T_T and f_T) of the damaged structure which are not actually used in the calculations. The latter are calculated assuming that all the springs have yielded, and their stiffness is described by the degraded value $k_{i,pl} = 0.1k_i$. The variation of the damping ratio with frequency is illustrated in Fig. 1, in which the vertical lines indicate the initial fundamental frequencies (continuous lines) and the tangent frequencies (dashed lines). The damping ratios based on the Rayleigh model are reasonably accurate only for the first three modes: for frequencies less than about 4 hz the error is less than 20%. On the contrary, the two damping matrices based on an optimal representation of a Caughey series, calculated without knowledge of the natural frequencies (except that required for a suitable choice of ω_{max}), resulted in stable damping ratios for all modes. As expected, the assumption that all floors are in the inelastic range leads to a dramatic reduction of all the natural frequencies. The Rayleigh damping approach would overestimate the damping ratio for the fundamental mode of the damaged structure by a factor of two, while the damping ratio for modes 2 to 7 would be close to the specified value. The *LSQM* approach, instead, would provide accurate damping ratios for the damaged structure for all modes. With the *LSQK* approach, the damping ratio for the fundamental mode of the damaged structure is reduced to about 1%, while for the higher modes it is very close to the specified value.

Table 1 – Properties of the example structure and damping ratios calculated with the three proposed approaches.

	Natural Periods and Frequencies				Damping ratios		
	Initial		Tangent				
Mode #	T_i (s)	f_i (hz)	T_T (s)	f_T (hz)	Rayleigh	LSQM	LSQK
1	1.00	1.00	3.16	0.32	0.050	0.048	0.047
2	0.39	2.57	1.23	0.81	0.050	0.050	0.049
3	0.24	4.11	0.77	1.30	0.066	0.050	0.050
4	0.18	5.58	0.57	1.77	0.085	0.050	0.050
5	0.14	6.97	0.45	2.20	0.103	0.050	0.050
6	0.12	8.31	0.38	2.63	0.121	0.050	0.050
7	0.10	9.63	0.33	3.05	0.139	0.050	0.050
8	0.09	10.95	0.29	3.46	0.157	0.050	0.050
9	0.08	12.27	0.26	3.88	0.175	0.050	0.050
10	0.07	13.59	0.23	4.30	0.193	0.050	0.050

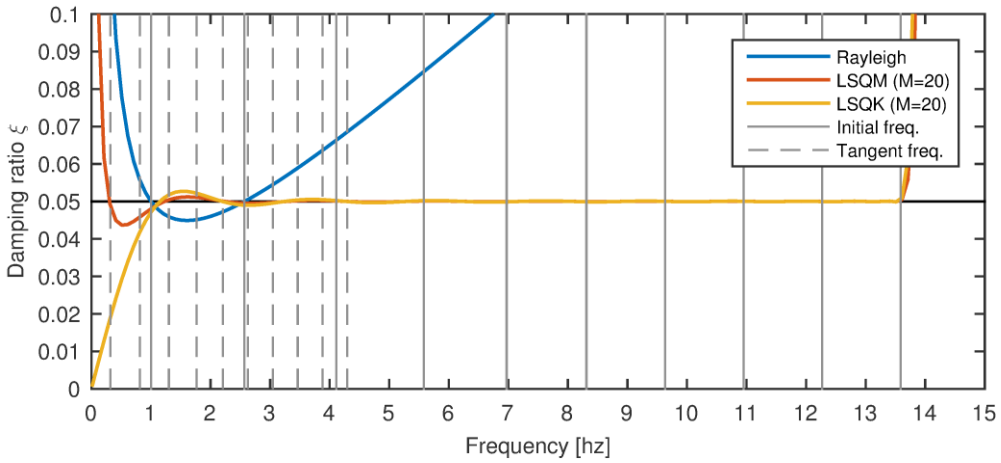

Fig. 1 – Variation of the damping ratio with frequency for the three damping models considered.

Three alternative damping models are considered. In the first model (labeled *Constant C*) the damping matrix is computed on the basis of the initial stiffness matrix, and this matrix is kept constant over the entire analysis. In the second model (labeled *Tangent damping*), the damping matrix is computed on the basis of the tangent stiffness matrix, and it is updated each time the latter changes. In the last model (labeled *Elastic velocity damping*) the damping matrix corresponds to the case *Constant C*, but the damping forces are calculated as described in Section 2. In the *Tangent damping* approach, the coefficients of the Rayleigh or Caughey series are kept constant and equal to those calculated with the initial structural properties.

The acceleration time-histories for two recorded ground motions are considered as seismic excitation. Both records are extracted from the PEER NGA-West 2 Database: (a) Northridge 1994 earthquake, recorded at Castaic-Old Ridge Route (RSN 963, 90° component), (b) Loma Prieta 1989 earthquake, recorded at Gilroy (RSN 767, 90° component). The two ground motions have been scaled in amplitude so that the 5% damped acceleration response spectrum at T = 1 s has a value $S_a(1)$ = 1 g. The scale factors for the two records are, respectively, 1.869 and 2.618. Fig. 2 shows the scaled time-histories of acceleration and velocity for the two records, together with their acceleration and velocity response spectra. The scaled records (a) and (b) have similar PGA (about 1 g) and maximum spectral acceleration (about 3.7 g), but they have very different spectral ordinates for periods longer than 1 s (larger acceleration for record b) and in the vicinity of T = 0.4 s (larger acceleration for record a). Since the first two natural modes of the elastic structure have periods of 1 s and 0.4 s, it can be expected that the different frequency content of the two records will have a different impact on the structural response. Record (b) is classified as a near-fault, pulse-like signal, with the period of the velocity pulse being about 2s.

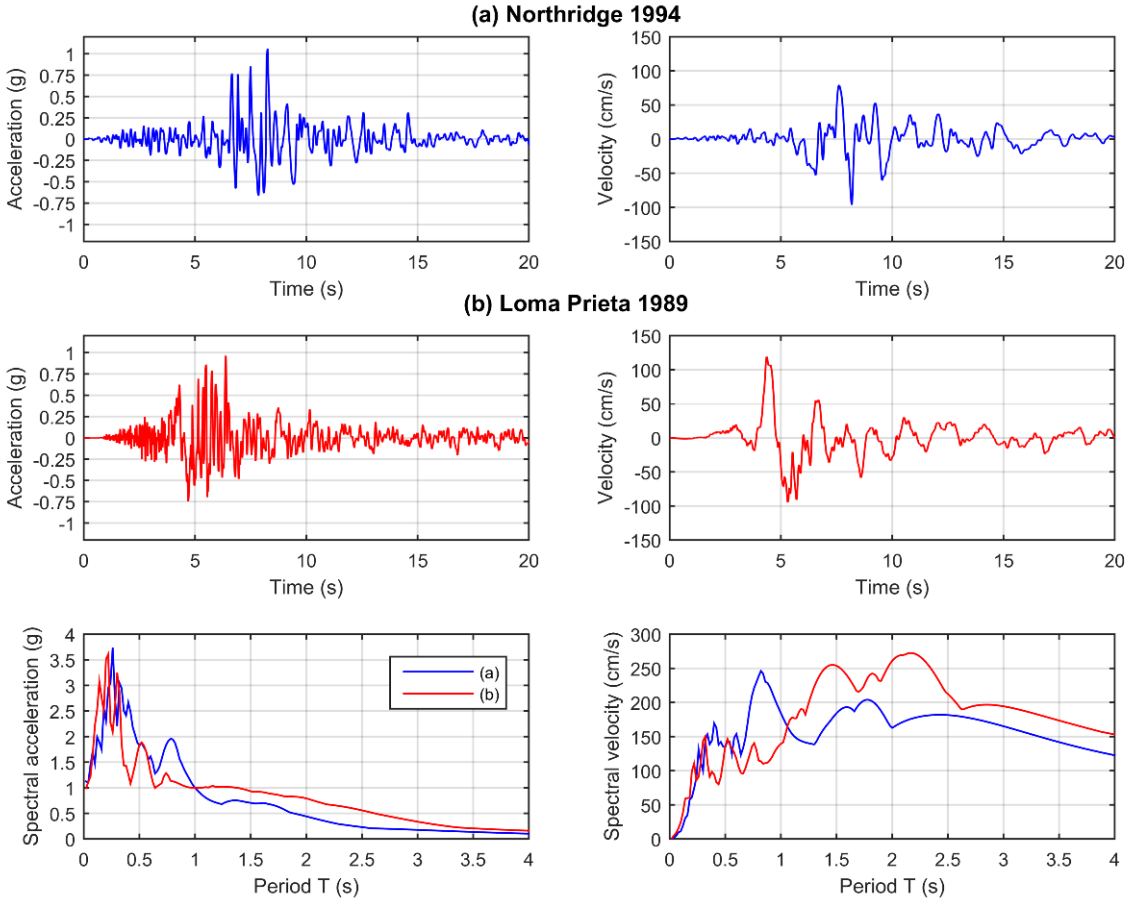

Fig. 2 – Acceleration and velocity time-histories and response spectra of the scaled ground motions

The time-history response of the ten-story model has been calculated by direct integration of the equations of motion through Newmark's constant acceleration method, using a time step Δt = 0.005 s in the interval 0 to 20s. The non-linear equations have been solved iteratively through a standard Newton-Rhapson scheme; convergence is assumed to be achieved when the energy increment is less than 10^{-5}. A comparison of the maximum absolute values, over time, of some response quantities is presented in Tables 2 and 3. A total of 20 analyses have been performed, varying the damping matrix (Rayleigh, Modal, LSQM and LSQK) and the technique used for calculating the damping forces (*Constant C*, *Tangent C* and *Elastic velocity damping*). For the modal damping model, only the *Constant C* approach was considered. The response quantities that are compared are: displacement, velocity and absolute acceleration of the last and first floor; shear at the base and at the last floor; viscous damping force at the first node and total viscous damping force; total "input" energy; energy dissipated by the hysteretic mechanism; and energy dissipated by inherent damping; normalized analysis time (set to unit for the *Constant C*, Rayleigh damping model).

Table 2 – Maximum response values for record (a) (Northridge, 1994-Castaic).

Record A		Constant C				Tangent damping			Elastic velocity damping		
Response parameter		Rayleigh	LSQM	LSQK	Modal	Rayleigh	LSQM	LSQK	Rayleigh	LSQM	LSQK
Top story displacement	[mm]	260.7	259.9	260.9	257.9	269.8	295.2	306.3	308.4	310.7	311.1
Top story velocity	[cm/s]	136.1	137.3	137.4	137	135.6	138.6	139.5	137.9	139.2	139.2
Top story abs. acceleration	[g]	0.546	0.551	0.551	0.55	0.515	0.555	0.564	0.529	0.551	0.552
Top story shear	[KN]	1791	1839	1840	1838	1820	1899	1897	1850	1936	1936
First story displacement	[mm]	58.5	61.4	61.5	61.2	66.5	67.8	68.6	70	70.4	70.4
First story velocity	[cm/s]	30.6	34.8	34.8	34.6	39.4	39.8	40.3	41	40.9	41
First story abs. acceleration	[g]	1.222	1.54	1.541	1.539	1.436	1.629	1.645	1.526	1.707	1.707
Base shear	[KN]	8666	8871	8878	8857	9232	9324	9380	9484	9509	9511
First node dissipative force	[KN]	963	491	492	490	839	411	412	843	363	363
Total dissipative force	[KN]	2195	1984	1957	2040	1600	1529	1505	1584	1508	1486
Input energy	[KN-m]	7047	7043	7033	7067	6951	6737	6633	6664	6674	6671
Energy dissipated by hysteresis	[KN-m]	4631	4759	4777	4723	4865	5151	5258	5134	5240	5254
Energy dissipated by inherent damping	[KN-m]	2416	2283	2255	2344	2086	1585	1374	1530	1434	1417
Normalized analysis time	[-]	1.00	1.00	1.00	1.00	1.20	10.17	10.26	1.07	1.08	1.08

Table 3 – Maximum response values for record (b) (Loma Prieta, 1989-Gilroy).

Record B		Constant C				Tangent damping			Elastic velocity damping		
Response parameter		Rayleigh	LSQM	LSQK	Modal	Rayleigh	LSQM	LSQK	Rayleigh	LSQM	LSQK
Top story displacement	[mm]	501.8	508.9	511.4	503.2	540.1	605.4	632.1	632.6	635.3	636.3
Top story velocity	[cm/s]	144.4	143.4	143.6	142.8	142.2	145.5	146	145	145.1	145.3
Top story abs. acceleration	[g]	0.511	0.512	0.511	0.514	0.524	0.508	0.5	0.494	0.5	0.5
Top story shear	[KN]	1559	1610	1611	1608	1682	1669	1668	1644	1672	1673
First story displacement	[mm]	89.5	90.2	90.5	89.6	93.9	98.9	101.6	100.7	100.1	100.2
First story velocity	[cm/s]	43.6	48.4	48.4	48.3	52.3	52.6	52.6	52.9	52.9	53
First story abs. acceleration	[g]	0.915	0.834	0.835	0.832	0.895	0.951	0.878	0.873	0.827	0.824
Base shear	[KN]	10872	10919	10939	10879	11181	11540	11734	11666	11622	11628
First node dissipative force	[KN]	984	517	517	518	558	257	235	530	264	264
Total dissipative force	[KN]	2805	2476	2444	2545	1625	1092	1124	1384	1270	1252
Input energy	[KN-m]	11067	11093	11116	11042	11184	11561	11608	11526	11544	11555
Energy dissipated by hysteresis	[KN-m]	7930	8105	8157	7991	8598	9715	10092	10058	10180	10210
Energy dissipated by inherent damping	[KN-m]	3133	2984	2955	3047	2582	1843	1414	1465	1361	1343
Normalized analysis time	[-]	1.00	1.02	1.02	1.02	1.21	9.87	8.18	1.12	1.14	1.15

Comparisons of the peak response quantities listed in Tables 2 and 3 lead to the following conclusions:

Constant C Models: (i) As expected the results based on full Caughey series (LSQM and LSQK) are similar to each other and to those obtained by use of a modal damping matrix. This represents a validation of the optimal

procedure to obtain full Caughey series. Significant differences between LSQM and LSQK are expected only when an updated stiffness matrix is used in the calculation. (ii) The response quantities more sensitive to the lower frequencies (roof displacements and velocity, base shear) are not very affected by the choice of damping matrix, while those more sensitive to higher frequencies (first story acceleration and velocity, dissipative forces) show more significant differences. This result is clearly related to the better representation of inherent damping for the higher modes allowed by a full Caughey series, and (iii) The first node damping force is 47 to 49% lower when a full damping matrix is used instead of Rayleigh damping.

Tangent Damping Models: (i) When the damping matrix is updated according to the changes of structural stiffness results are instead very sensitive to the choice of the damping matrix. For earthquake (b), the roof displacements obtained with an updated LSQM and LSQK damping matrix are respectively 12% and 17% higher with respect to the updated Rayleigh damping case. The corresponding first node damping forces are 51 to 58% lower than when Rayleigh damping is used. (ii) Most of the results obtained by the LQSK approach are slightly higher than those obtained by the LSQM approach as a result of the reduction of the first mode damping ratio shown in Fig. 1. (iii) The use of updated properties (Tangent damping) leads to significantly higher responses than when initial properties (Constant C) are used. For earthquake (b), the roof displacement is higher by 8, 19 and 24%, respectively, when updated properties are used in conjunction with the Rayleigh, LSQM and LSQK approaches. Larger deviations are obtained for other parameters, such as 43 to 55% reduction for the damping force at the first node, and (iv) use of the tangent damping model in combination with full damping matrices required a much longer computational time (maximum 10 times higher). This time can be reduced as the present code could be optimized. For example, at the moment, when a tangent approach is used, the damping matrix is recalculated at each analysis step, irrespective of the fact that the stiffness matrix had changed or not.

Elastic Velocity Damping Model: (i) The results based on full Caughey series (LSQM and LSQK) are similar to each other and to those obtained by use of a modal damping matrix (not shown for brevity), (ii) With exception of the damping force on the first node which can be 50 to 57% smaller, the results based on the LSQM and LSQK matrices are similar to those obtained by use of a Rayleigh damping matrix, (iii) The peak displacement and base shear response for the LSQM and LSQK elastic velocity model are similar to those for the corresponding tangent models but are significantly larger than those based on the initial properties, and (iv) The elastic velocity model is very efficient requiring only 15% more computational time than the constant Rayleigh damping model.

The plot in Fig. 3 shows the time-history of the total velocity at the first node and of the velocity of the elastic component of the displacement obtained as described in Section 2. The plot refers to the Elastic velocity damping with LSQK damping matrix subject to earthquake (b). It can be observed that the "elastic" velocity is equal to the total velocity when the amplitude of the response is small at the beginning of the time-history (before the strong motion phase) and also at the end of the motion.

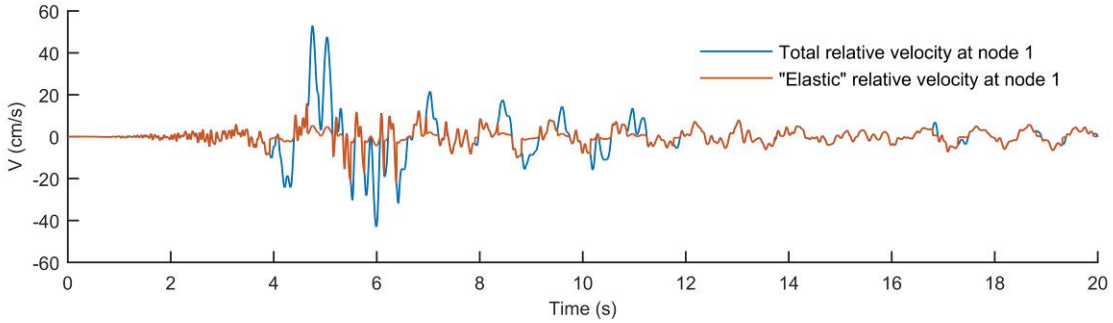

Fig. 3 – Time history (0-20 s) of the total velocity and of the "elastic" velocity at node 1. Earthquake (b), "elastic" velocity LSQK damping model.

The plots in Fig. 4 and 5 show the time-history (first 10 seconds) of the base shear and total dissipative force of the structure subjected to earthquake (b). A comparison is presented between the constant modal damping matrix, the tangent and the elastic velocity LSQK models. While the time history of the base shear is

not greatly affected by the damping model, the total dissipative force is greatly affected by it. During the nonlinear response phase, the peak of the total damping force equals 56% of the yield strength of the first story when a constant damping matrix is used. If the damping matrix is updated or if the elastic velocity damping is used, the peak reduces to 26% of the first story strength.

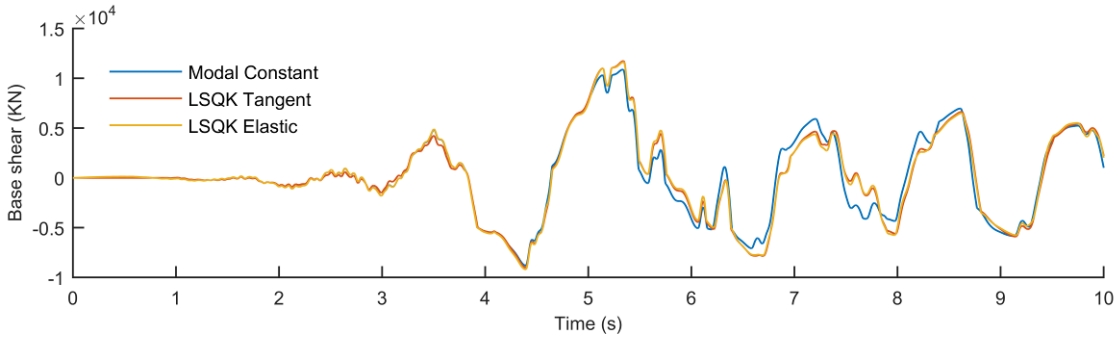

Fig. 4 – Time history (0-10 s) of the base shear for earthquake (b), comparison between constant modal damping matrix, tangent LSQK damping model and "elastic" LSQK damping model.

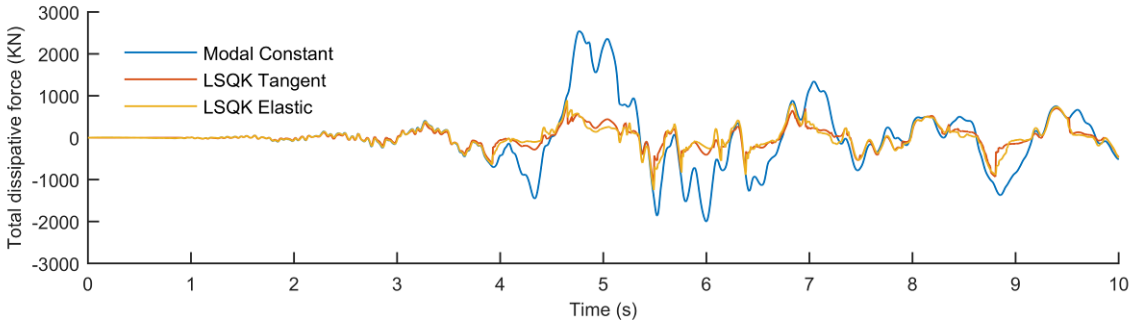

Fig. 5 – Time history (0-10 s) of the total dissipative force for earthquake (b), comparison between constant modal damping matrix, tangent LSQK damping model and "elastic" velocity LSQK damping model.

4. Base-Isolated Structures

As a second example, we consider the same ten story building model analyzed in section 3, now supported on a nonlinear base-isolation system. The mass and stiffness properties of the superstructure are left unchanged, but one additional degree of freedom represents the slab above the isolators, which has a mass $m_0 = m$, equal to the floor masses. The isolator system is represented by a bilinear mechanism with initial stiffness $k_{is,1} = 0.20k_1$, where k_1 is the stiffness of the first story, degraded stiffness $k_{is,2} = 0.1k_{is,1}$ and yield strength $F_{is,y}$ = 1834 KN, corresponding to about 5% of the total weight of the structure (including the mass of the slab). The yield displacement of the isolator is x_0 = 1.29 cm. Added viscous damping characterized by a damping constant $c_{ad} = 2 \cdot \xi_{ad} (4 \cdot m \cdot k_{is,1})^{0.5}$, in which ξ_{ad} =5% is provided in the isolator system.

We select to use the standard step-by-step numerical formulation in terms of the relative displacements (u_0, u_i) (i=1,10) with respect to the moving ground surface (below the isolators), in which u_0 is the deformation of the isolator. In this formulation, it is necessary to assemble the global damping matrix

$$[C_{global}] = [C_{ad}] + [C_s] = \left[\begin{array}{c|c} c_{ad} & \{0\}^T \\ \hline \{0\} & [0] \end{array}\right] + [C_s] \tag{10}$$

in which $[C_s]$ is the damping matrix for the unrestrained superstructure (including the mass m_0 above the isolators). It should be noted that the global damping matrix may not be classical.

Hall [8] and Ryan and Polanco [9] have shown that the mass proportional term in a Rayleigh damping matrix leads to unrealistic results in the case of base-isolated structures. For this reason, we use the LSQK

expansion without the mass proportional term for $[C_s]$ in which the matrices $[m]$ and $[\bar{k}]$ are calculated for the unconstrained superstructure. A series of order M = 14 is used with $\omega_{max} = 2(k_1/m)^{0.5} = 91.5$ rad/s, which is an upper bound of the maximum frequency for this type of structure.

Table 4 lists the natural frequencies (f_u) and obtained modal damping ratios (ξ_u) for the unconstrained superstructure model. It is clear that the damping matrix proposed leads to a very good agreement between the target and the calculated damping ratios. Table 4 also lists the initial natural frequencies ($f_{is,i}$) and the approximate modal damping ratios (ξ_{is}) of the isolated structure; the latter are calculated as the diagonal terms of the reduced modal damping matrix (which is not diagonal in this case) for three values of added damping (ξ_{ad}) in the isolators (although only the case ξ_{ad}=5% is considered in the rest of the paper). Also included in Table 4 is an estimate of the "tangent" natural frequencies ($f_{is,t}$), obtained by assuming that the stiffness of the isolators corresponds to the degraded value $k_{is,2}$.

Table 4 – Natural frequencies and modal damping ratios for the unconstrained and isolated systems.

Mode #	Unconstrained superstructure		Isolated structure				
i	f_u (hz)	ξ_u (%)	Initial freq. $f_{is,i}$ (hz)	Tangent freq. $f_{is,t}$ (hz)	Approximate modal damping ratio ξ_{is} (%) ξ_{ad} = 0	ξ_{ad} = 5%	ξ_{ad} = 10%
1	0.00	0.00	0.73	0.30	0.80	2.70	4.60
2	1.73	4.96	2.04	1.77	4.10	6.50	8.90
3	3.24	5.04	3.44	3.26	4.70	6.60	8.50
4	4.70	4.96	4.84	4.72	4.80	6.20	7.60
5	6.10	5.03	6.19	6.10	4.90	6.00	7.10
6	7.42	4.97	7.49	7.43	4.90	5.70	6.60
7	8.70	5.03	8.76	8.71	5.00	5.60	6.30
8	9.98	4.98	10.02	9.98	5.00	5.50	6.00
9	11.24	5.01	11.28	11.24	5.00	5.40	5.80
10	12.50	5.00	12.52	12.50	5.00	5.30	5.60
11	13.73	4.99	13.75	13.73	5.00	5.20	5.30

The response of the isolated structure subjected to a harmonic horizontal ground acceleration $\ddot{u}_g = A\sin(\omega_f\, t)$ was computed by direct integration for several values of excitation frequency and amplitude. The duration of the input acceleration (number of cycles) was selected so that stationary conditions were reached and the integration time step was set between 1/100 and 1/200 of the period of the excitation ($T_f = 2\pi/\omega_f$).

First, it was assumed that the superstructure has infinite strength and remains in the linear range, so that the effects of inherent damping can be accounted for by using a constant damping matrix. The plot in Fig. 6a shows the frequency response functions for the base slab (above the isolators) of the building (i.e. the amplitude of the normalized harmonic displacement at the first degree of freedom as a function of the excitation frequency), calculated for different values of the excitation amplitude A. The plot clearly shows that for sufficiently high excitation amplitudes, resonance occurs at a frequency of 0.295 hz. For an amplitude A=0.10g, the ductility response is U_0/x_0 = 33. These results are in excellent agreement with the approximate analytical expressions provided by Luco [17] for a 1-DOF linear structure on a bilinear isolator on rigid soil, which would predict a resonant frequency of 0.296 hz and a maximum ductility for A = 0.10g of U_0/x_0 = 34.

Then, we consider the case in which the superstructure as a finite strength, corresponding to that described in section 3. In this case, for sufficiently high excitation amplitudes both the isolator and the superstructure yield, and the effect of the inherent damping model can be of relevance. Fig. 6b shows the frequency response curves for the base slab (U_0/x_0) [with x_0 = 1.29 cm] and the top of the building (U_{10}/x_{10}) [with x_{10} = 8.29 cm corresponding to the roof yield displacement] for an excitation amplitude A = 0.20g obtained with the *Constant C* and the *Elastic velocity damping* models. In the latter case, the dissipative force is calculated as $\{f_d\} = [C_s]\{\dot{u}_e\} + [C_{ad}]\{\dot{u}\}$, where $\{\dot{u}\}$ and $\{\dot{u}_e\}$ are, respectively, the total relative velocity and the "elastic" velocity vectors.

Results indicate that the resonant frequency is reduced to 0.225 hz with respect to the elastic superstructure case (0.295 hz), and that the two damping models can lead to significant differences in the

calculated response. The maximum ductility of the isolators obtained with the Elastic velocity damping model (115.8) is 34% higher than that given by the Constant C model (86.7). The normalized displacement of the roof (U_{10}/x_{10},) shows a 43% increase from 28.4 (Constant C) to 40.6 (Elastic velocity damping).

Even though structural properties and excitation levels were selected with the aim of reproducing realistic situations, the calculated harmonic response is clearly too high for a real structure. It is reasonable to expect that the transient response to an actual earthquake motion will be limited due to the short duration of the various harmonic components of the signal. The important investigation of the effects of the critical excitation on the transient response of base-isolated structures is currently underway.

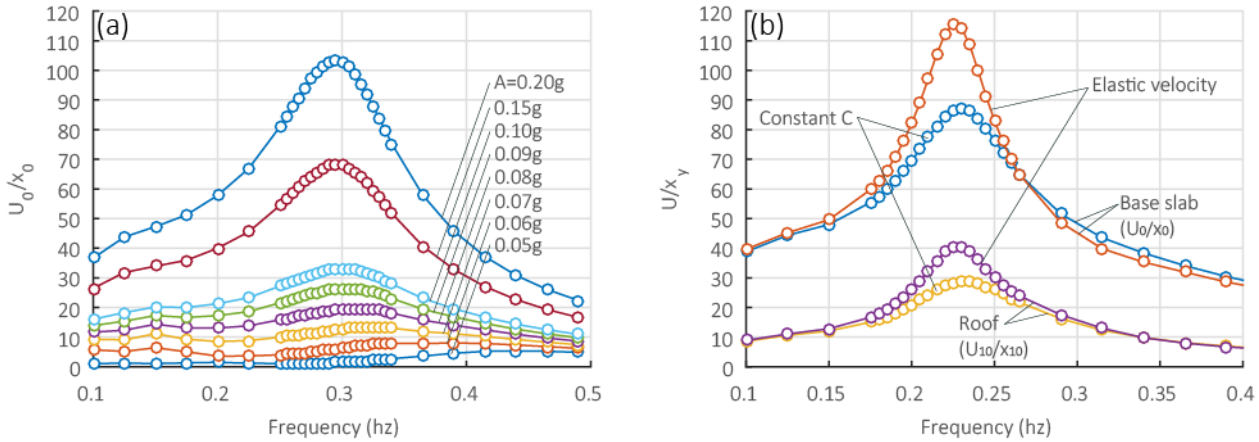

Fig. 6 – Frequency response functions of the isolated ten-story building model: (a) elastic superstructure, ductility response at the base (U_0/x_0); (b) inelastic superstructure, ductility response at the base (U_0/x_0) and at the top (U_{10}/x_{10}) for A=0.20g and comparison of *Constant C* and *Elastic velocity damping* models.

5. Conclusions

(1) A new model for the inherent damping force which depends on an estimate of the "elastic" component of velocity rather than the total velocity, which includes elastic and plastic components, has been presented. The proposed damping model [Eq. (7)] is such that: (i) it reduces to the standard model in the linear case, (ii) the damping forces are mostly associated with loading and unloading, (iii) the inherent damping is clearly separated from the hysteretic damping due to inelastic action, (iv) there is no remnant inherent damping force at the end of the structural motion, and (v) the calculation can be done efficiently and does not represent a significant additional burden. In fact, the new approach takes less computational time than the use of Rayleigh damping with a tangent stiffness matrix. In addition, if the damping matrix $[c]$ in Eq. (7) is based on Eq. (2b) as suggested by Bernal [4], or by the modal approach [Eq. (3)] as suggested by Carr [5] and Chopra and McKenna [15], or by use of Eq. (4b), then the damping forces at massless degrees of freedom would be zero.

(2) Analyses of the calculated seismic inelastic response of a 10-story building with different models of the inherent damping indicate that the proposed new damping model leads to results similar to those obtained by use of viscous models based on the instantaneous tangent stiffness, and to a significantly larger response than that obtained by standard viscous models (Rayleigh, optimized Caughey series, Modal damping matrix) based on the initial structural properties. The new model leads to 10 to 25% more energy dissipated by hysteresis depending on the seismic excitation, and to a reduction of 37 to 55% of the energy dissipated by inherent damping.

(3) The optimized Caughey series obtained by the authors ([22], [23]) to obtain a viscous damping matrix represent a significant improvement over the Rayleigh damping matrix for analyses using the initial and degraded structural properties. However, there is a significant additional computational cost to the Caughey series approach when the instantaneous tangent stiffness is used.

(4) It has been confirmed numerically that a harmonic critical excitation exists for a multi-story structure supported on a bilinear hysteretic isolator system. This extends the analytical findings for a simple bilinear

oscillator (Caughey [16]) and for a 1-DOF structure resting on a bilinear hysteretic isolator (Luco [17]), that even in the presence of hysteretic damping, a critical amplitude of the harmonic excitation exists, beyond which the resonant response of the structure can be unbounded. The role of the viscous damping model on the response at the critical excitation was examined.

6. References

[1] Chrisp, DJ (1980): Damping models for inelastic structures, *MS thesis*, Univ. of Canterbury, Christchurch, New Zealand.
[2] Shing PB, Mahin SA (1987): Elimination of spurious higher-mode response in pseudodynamic tests, *Earthquake Engineering and Structural Dynamics*, **15**, 425-445.
[3] Leger P, Dussault S (1992): Seismic-energy dissipation in MDOF structures, *ASCE Journal of Structural Engineering*, **118**(6),1251-1267.
[4] Bernal D (1994): Viscous damping in inelastic structural response, *ASCE Journal of Structural Engineering*, **120**(4),1240-1254.
[5] Carr AJ (1997): Damping models for inelastic structures, *Proc. Asia-Pacific Vibration Conference*, Kyongju, Korea, Vol. 1, 42-48.
[6] Carr AJ (2005): Damping models for time-history structural analyses, *Proc. Asia-Pacific Vibration Conference*, Langkawi, Malaysia, 287-293.
[7] Carr AJ (2007): Ruaumoko Manual, Vol 1: Theory and User's Guide to Associated Programs, University of Canterbury, Christchurch, New Zealand.
[8] Hall JF (2006): Problems encountered from the use (or misuse) of Rayleigh damping, *Earthquake Engineering and Structural Dynamics*, **35**, 525-545.
[9] Ryan KL, Polanco J (2008): Problems with Rayleigh Damping in Base-Isolated Buildings, *ASCE Journal of Structural Engineering*, **134**(11),1780-1784.
[10] Charney FA (2008): Unintended consequences of modeling damping in structures, *ASCE Journal of Structural Engineering*, **134**(4):581-592.
[11] Petrini L, Maggi C, Priestley N, Calvi M (2008): Experimental verification of viscous damping modeling for inelastic time history analyses, *Journal of Earthquake Engineering*, **12**(1), 125–145.
[12] Zareian F, Medina RA (2010): A practical method for proper modeling of structural damping in inelastic plane structural systems, *Computers and Structures*, **88**,45-53.
[13] Smyrou E, Priestley MJN, Carr AJ (2011): Modelling of elastic damping in nonlinear time-history analyses of cantilever RC walls, *Bull. Earthquake Eng*., **9**(5),1559-1578.
[14] Jehel P, Leger P, Ibrahibegovic A (2014): Initial versus tangent-stiffness based Rayleigh damping in inelastic time history analysis, *Earthquake Engineering and Structural Dynamics*, **43**, 476–484.
[15] Chopra AK, McKenna P (2016): Modeling viscous damping in nonlinear response history analysis of buildings for earthquake excitation, *Earthquake Engineering and Structural Dynamics*, 45, 193-211.
[16] Caughey TK (1960): Sinusoidal excitation of a system with bilinear hysteresis, *ASME Journal of Applied Mechanics*, 28 EM2, 131-66.
[17] Luco JE (2014): Effects of soil-structure interaction on seismic base isolation, *Soil Dynamics and Earthquake Engineering*, **66**, 167-177.
[18] Caughey TK (1960): Classical normal modes in damped linear dynamic systems, *ASME Journal of Applied Mechanics*, **27**, 269-271.
[19] Caughey TK, O'Kelly MEJ (1965): Classical normal modes in damped linear dynamic systems, *ASME Journal of Applied Mechanics*, **32**(3), 583-588.
[20] Wilson EL, Penzien J: Evaluation of orthogonal damping matrices, *International Journal for Numerical Methods in Engineering*, **4**, 5-10.
[21] Luco JE (2008): A note on classical damping matrices, *Earthquake Engineering and Structural Dynamics*, **37**, 615-626.
[22] Lanzi A, Luco JE (2016): Caughey damping series in terms of products of the flexibility matrix, submitted for publication
[23] Luco JE, Lanzi A (2015): Optimal Caughey series representation of classical damping matrices, submitted for publication.
[24] Luco JE (2008): Author's reply: A note on classical damping matrices, *Earthquake Engineering and Structural Dynamics*, **37**(15), 1805-1809.